

# ADVANCED ENERGY MATERIALS

## Supporting Information

for *Adv. Energy Mater.*, DOI: 10.1002/aenm.201600595

Toward High-Thermoelectric-Performance Large-Size  
Nanostructured BiSbTe Alloys via Optimization of Sintering-  
Temperature Distribution

*Gang Zheng, Xianli Su,\* Xinran Li, Tao Liang, Hongyao  
Xie, Xiaoyu She, Yonggao Yan, Ctirad Uher, Mercuri G.  
Kanatidis, and Xinfeng Tang\**

## Supporting Information

**Toward high thermoelectric performance large-size nanostructured BiSbTe alloys via optimization of sintering temperature distribution**

Gang Zheng, Xianli Su,\* Xinran Li, Tao Liang, Hongyao Xie, Xiaoyu She, Yonggao Yan, Ctirad Uher, Mercuri G. Kanatzidis, Xinfeng Tang\*

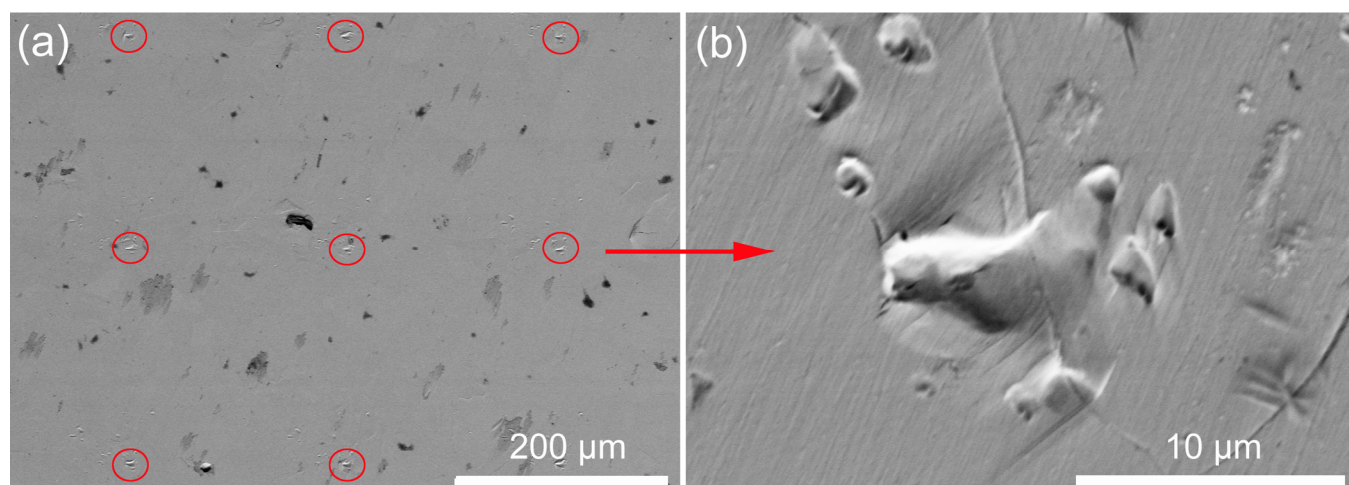


**Figure S1.** SEM image of the surface on which Seebeck coefficients were measured by the scanning Seebeck probe.

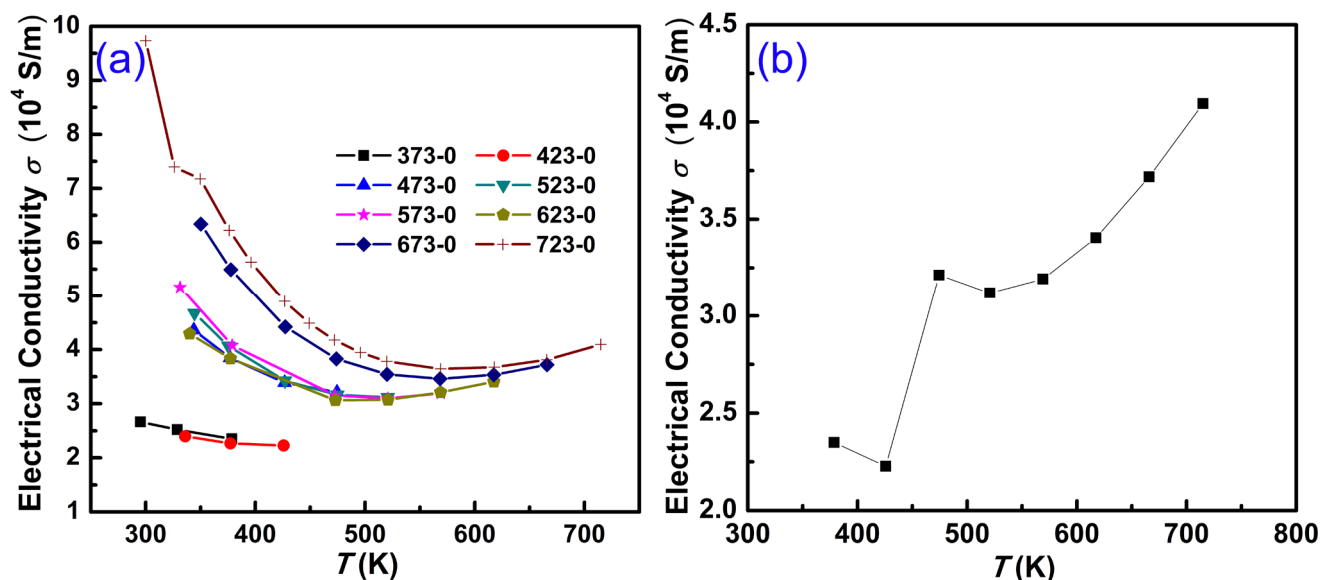


**Figure S2.** (a) Temperature dependence of the electrical conductivity for samples synthesized by MS-PAS at different sintering temperatures but with no holding time; (b) electrical conductivity measured at the sintering temperature for the samples synthesized by MS-PAS at different sintering temperatures but with no holding time.

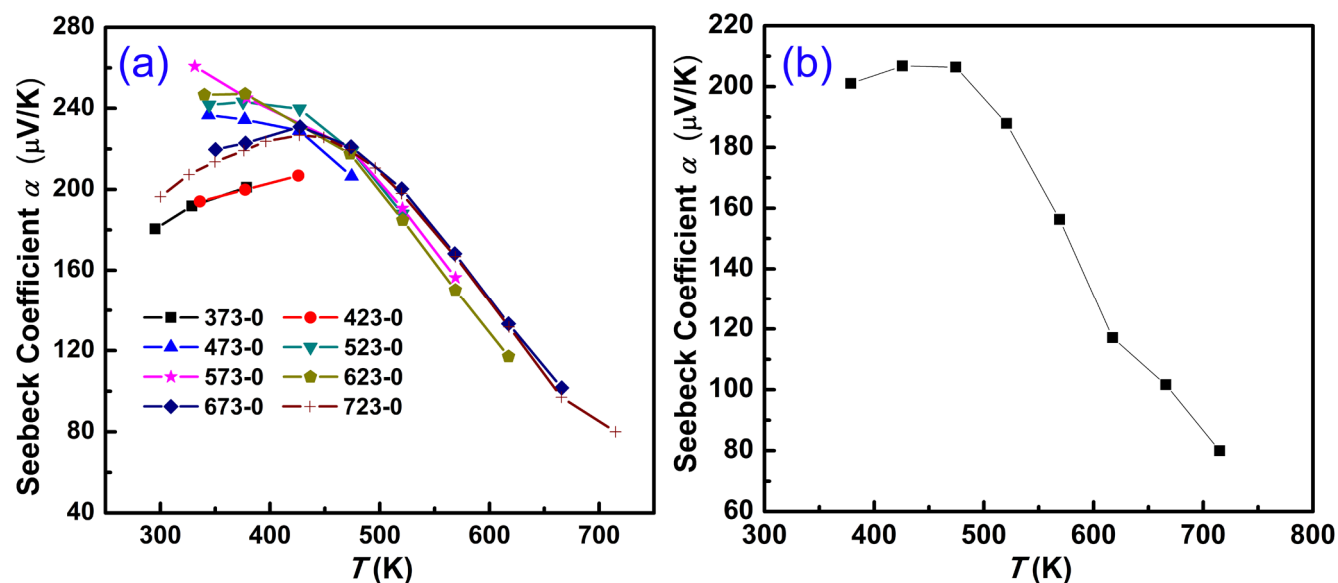


**Figure S3.** (a) The temperature dependence of the Seebeck coefficient measured on samples synthesized by MS-PAS at different sintered temperatures but with no holding time; (b) Values of the Seebeck coefficient measured at the sintering temperature for the samples synthesized by MS-PAS at different sintering temperatures but with no holding time.

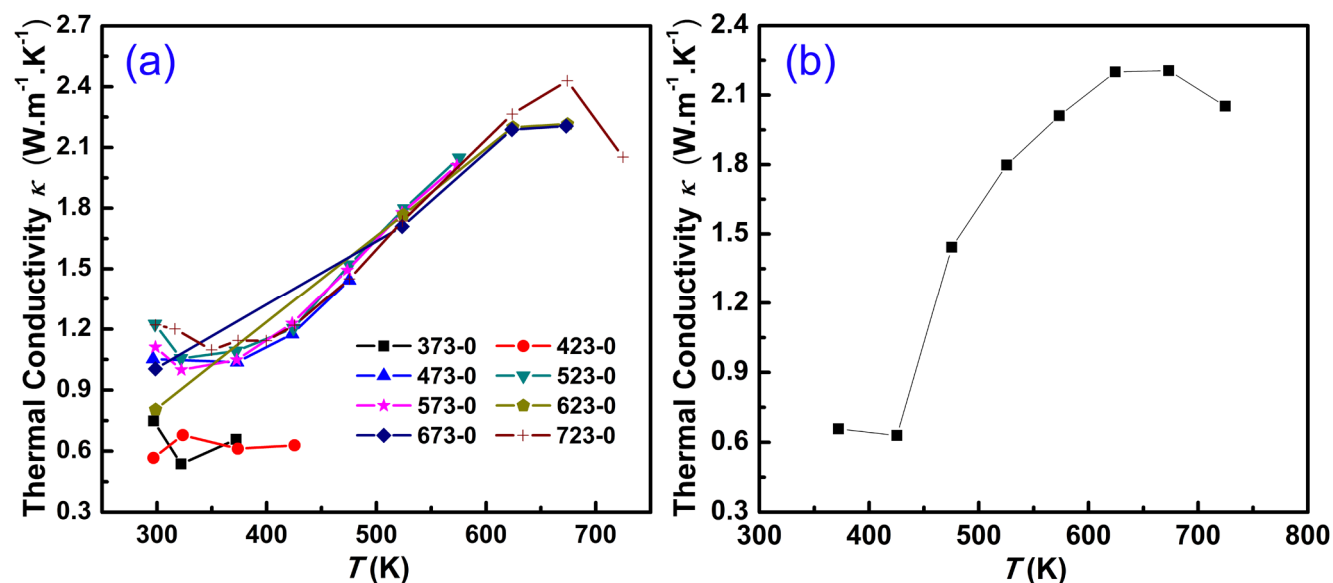


**Figure S4.** (a) Temperature dependence of the thermal conductivity measured on samples synthesized by MS-PAS at different sintering temperatures but with no holding time; (b) thermal conductivity measured at the sintering temperature for samples synthesized by MS-PAS at different sintering temperatures but with no holding time.

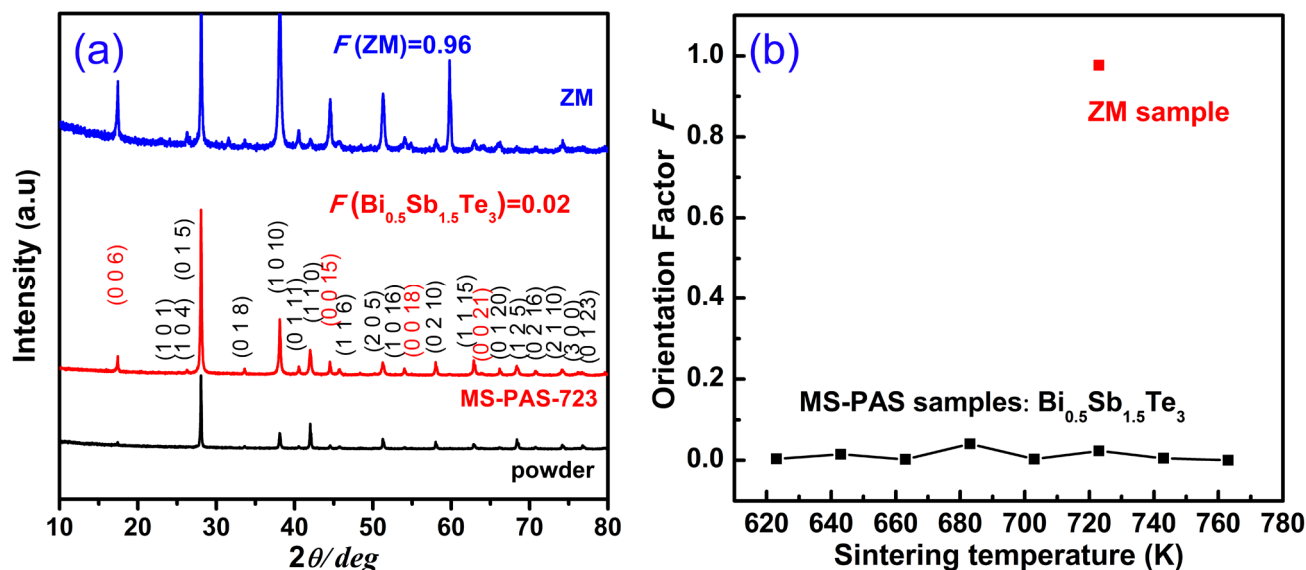


**Figure S5.** (a) Diffraction peak identification and the orientation factor calculation for a sample synthesized by MS-PAS and for the ZM sample. Black trace: powder after MS. Red trace: MS-PAS sample. Blue trace: ZM sample, reflections taken on the a–b plane; (b) relationship between the orientation factor and the sintering temperature for MS-PAS processed samples.

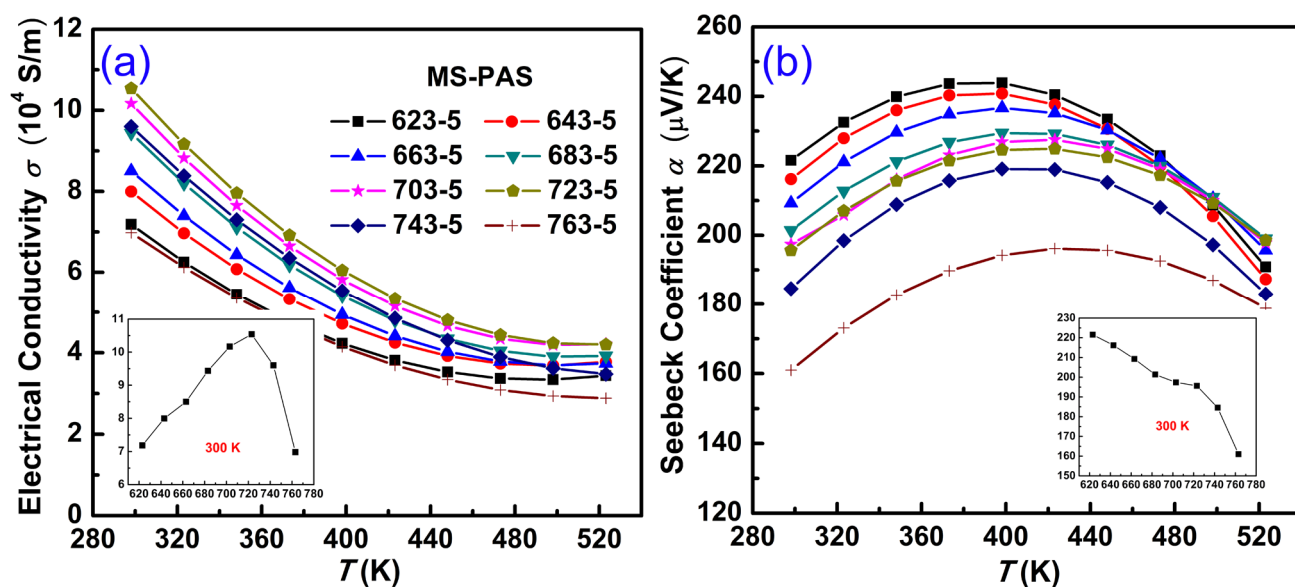


**Figure S6.** (a) Temperature dependence of the electrical conductivity for MS-PAS synthesized samples at different sintering temperatures between 623K and 763 K. The inset shows the sintering temperature dependence of the electrical conductivity at room temperature; (b) temperature dependence of the Seebeck coefficient for MS-PAS synthesized samples at different sintering temperatures between 623K and 763 K. The inset displays the sintering temperature dependence of the Seebeck coefficient at room temperature.

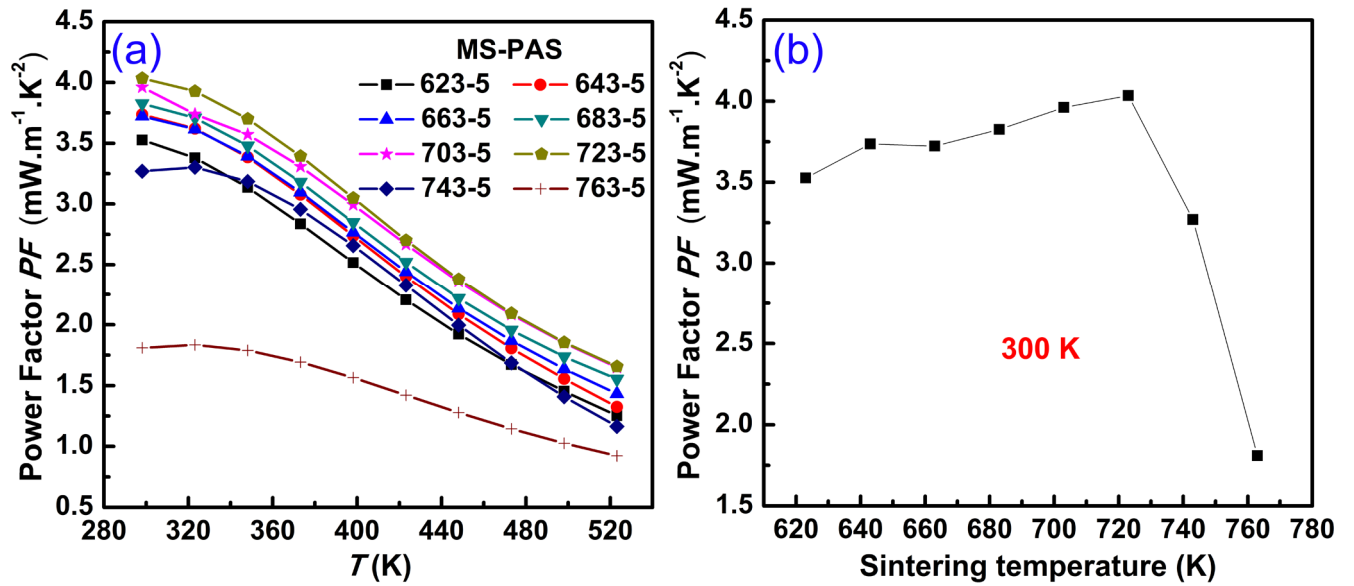


**Figure S7.** (a) Temperature dependence of the power factor for MS-PAS synthesized samples at different sintering temperatures between 623K and 763 K; (b) sintering temperature dependence of the power factor at room temperature.

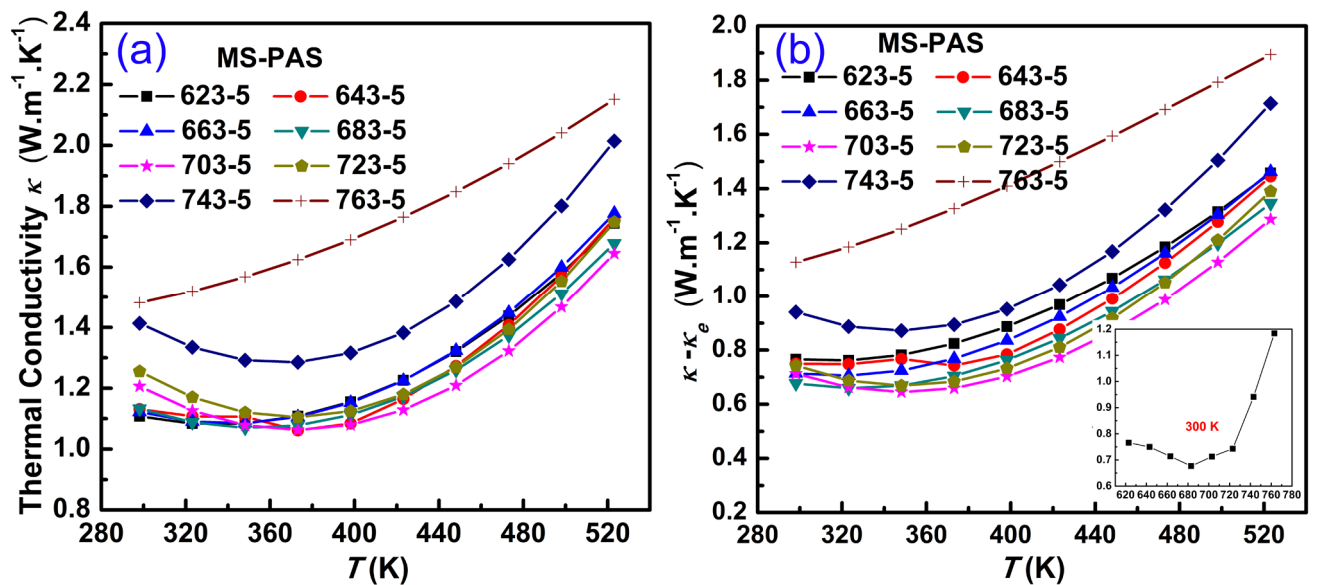


**Figure S8.** (a) Temperature dependence of the thermal conductivity for MS-PAS synthesized samples at different sintering temperatures between 623K and 763 K; (b) the temperature dependence of the lattice thermal conductivity,  $\kappa_L = \kappa - \kappa_e$ , for MS-PAS synthesized samples at different sintering temperatures between 623K and 763 K. The inset shows the sintering temperature dependence of  $\kappa_L = \kappa - \kappa_e$  at room temperature.

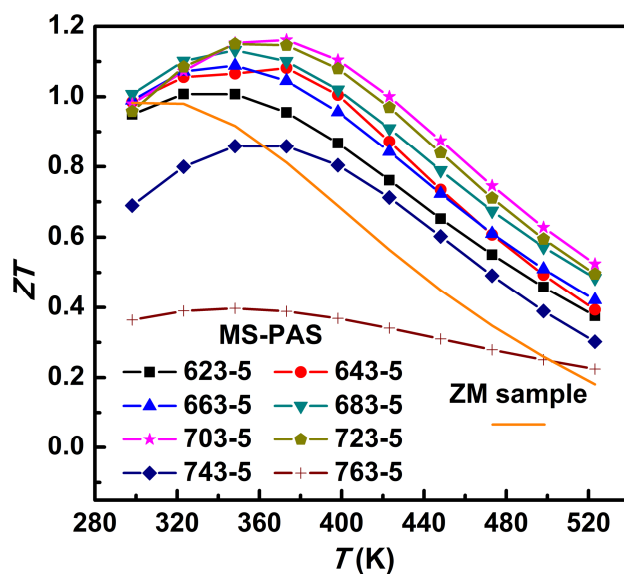


**Figure S9.** The temperature dependence of  $ZT$  for MS-PAS synthesized samples at different sintering temperatures between 623K and 763 K.

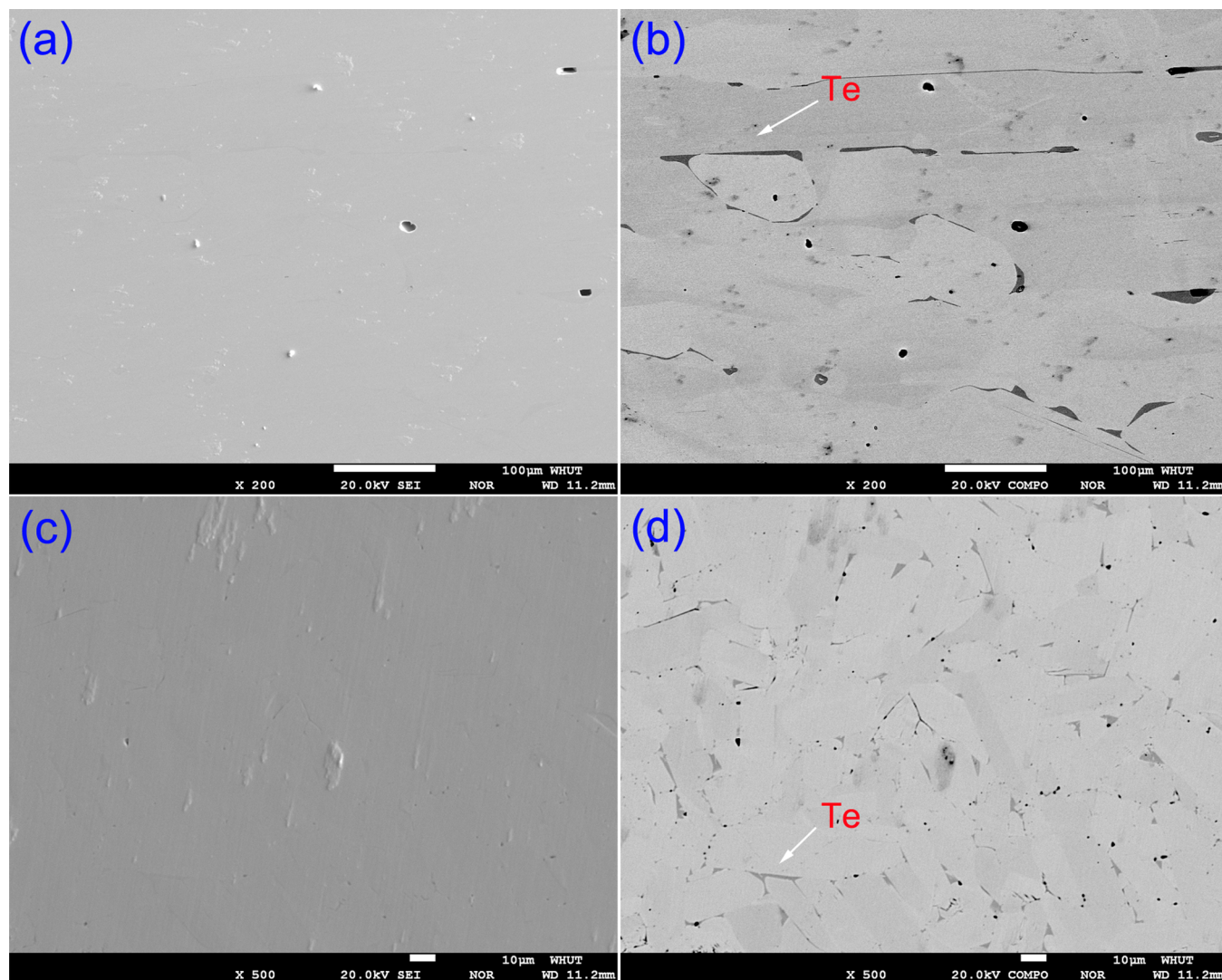


**Figure S10.** (a) BSE image of the ZM sample; (b) BSE image of the ZM sample; (c) BSE image of a sample cut from the ingot with the diameter of 30 mm and height of 12 mm and

sintered for 5 min; (d) BSE image of a sample cut from the ingot with the diameter of 30 mm and height of 12 mm and sintered for 5 min.

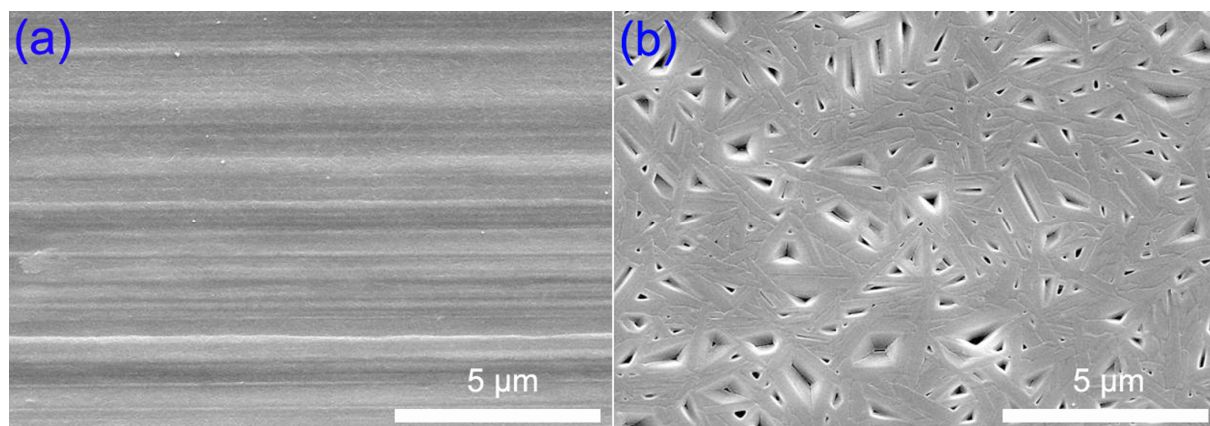


**Figure S11.** (a) SEM image of the contact surface of a ribbon prepared by MS; (b) SEM image of the free surface of a ribbon prepared by MS.

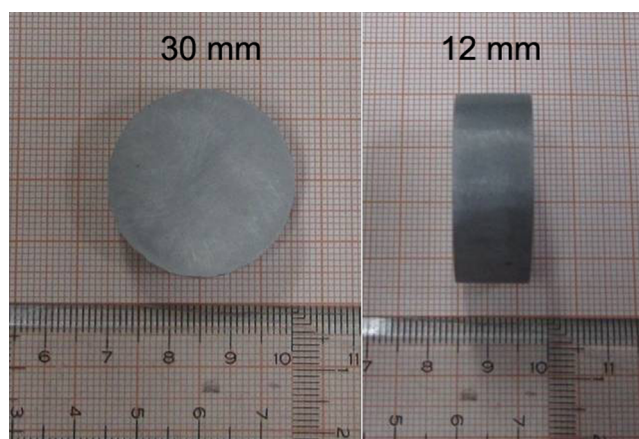


**Figure S12.** Images of an ingot with the diameter of 30 mm and height of 12 mm prepared by MS-PAS.